The local structure of OH species on the $V_2O_3(0001)$ surface: a scanned-energy mode photoelectron diffraction study

E. A. Kröger[1], D. I. Sayago[1], F. Allegretti[2×], M. J. Knight[2], M. Polcik[1♦], W. Unterberger[1], T. J. Lerotholi[2], K. A. Hogan[3], C. L. A. Lamont[3], M. Cavalleri[4], K. Hermann[4], D. P. Woodruff[2*]

[1] ***Chemical Physics Department, Fritz-Haber-Institut der Max-Planck-Gesellschaft, Faradayweg 4-6, 14195 Berlin, Germany***

[2] ***Physics Department, University of Warwick, Coventry CV4 7AL, UK***

[3] ***Dept. of Chemical & Biological Sciences, University of Huddersfield, Queensgate, Huddersfield HD1 3DH, UK***

[4] ***Theory Department, Fritz-Haber-Institut der Max-Planck-Gesellschaft, Faradayweg 4-6, 14195 Berlin, Germany***

Abstract

Scanned-energy mode photoelectron diffraction (PhD), using O 1s photoemission, together with multiple-scattering simulations, have been used to investigate the structure of the hydroxyl species, OH, adsorbed on a $V_2O_3(0001)$ surface. Surface OH species were obtained by two alternative methods; reaction with molecular water and exposure to atomic H resulted in closely similar PhD spectra. Both qualitative assessment and the results of multiple scattering calculations are consistent with a model in which only the O atoms of outermost layer of the oxide surface are hydroxylated. These results specifically

---

[×] present address: Karl-Franzens-Universität Graz, Institut für Physik, Bereich für Experimentalphysik, Universitätsplatz 5, 8010 – Graz, Austria

[♦] present address: ANF Data, AS IL W, Herspicka 5, 639 00, Brno, Czech Republic

[*] corresponding author, email: d.p.woodruff@warwick.ac.uk

exclude significant coverage of OH species atop the outermost V atoms, i.e. in vanadyl O atom sites. *Ab initio* density-functional theory cluster calculations provide partial rationalisation of this result, which is discussed the context of the general understanding of this system.

Keywords: Photoelectron diffraction; ab initio DFT; cluster approximation; surface structure; vanadium oxide; hydrogen; water

1. Introduction

Oxide surfaces in general, and those of vanadium oxides in particular, play a major role in practical heterogeneous catalysis [1]. As such there have been many investigations of model oxide surfaces using surface science methods, although very few of these have involved quantitative surface structure determination, and even fewer have led to quantitative information on adsorbate structures. A particularly interesting problem in understanding the role of oxides in surface reactions is the influence of surface hydroxyl (OH) species. Some published literature suggests that hydroxyl termination of oxide surfaces is ubiquitous, particularly in aqueous environments, but also when exposed to air at atmospheric pressure. Insofar as some oxides have potential applications as catalysts in hydrogen production by water dissociation, surface hydroxyl species may also play a direct role in at least one important surface reaction.

Here we present the results of an investigation of the local structure of OH species on the $V_2O_3(0001)$ surface, produced either by water dissociation or by reaction with atomic hydrogen, using the quantitative structural technique of scanned-energy mode photoelectron diffraction (PhD) [2, 3]. As in almost all recent studies of $V_2O_3(0001)$, this work was conducted on epitaxial films of the oxide grown *in situ*. This method of preparing the surface overcomes the complications of producing well-ordered stoichiometric surfaces on bulk oxide samples and is well-established for V_2O_3. In particular, well-ordered $V_2O_3(0001)$ films, as characterised by their low energy electron diffraction (LEED) pattern, have been grown on a range of substrates including W(110) [4], $Cu_3Au(100)$ [5], Au(111) [4], Pd(111) [6, 7, 8, 9, 10] and Rh(111) [11, 12, 13], and here we followed the methodology established for growth on Pd(111). As a complement to this experimental structure determination we also present the results of *ab initio* density-functional theory (DFT) cluster calculations of the principle structural models discussed.

At room temperature the bulk structure of vanadium sesquioxide, V_2O_3, is trigonal (space group $R\bar{3}c$, no. 167) and can be represented by a hexagonal unit cell with lattice

parameters of a=14.00 Å and c=4.95 Å containing six V_2O_3 units [14]. Relative to the (0001) basal plane, the structure, like that of corundum (Al_2O_3), comprises alternate buckled layers containing 2 metal atoms per unit mesh and planar layers containing 3 oxygen atoms per unit mesh, this layer structure being denoted here as ….VOV'VOV'….. The O layers are laterally distorted relative to a true close-packing, and the nearest V atoms occupy three-fold coordinated sites relative to these O atom layers. This bulk structure allows three intrinsic (0001) bulk terminations, the oxygen terminated OVV' and the full metal terminated VV'O polar surfaces and a less polar half metal layer termination with only one of the two vanadium layers being topmost, denoted as V'OV. In this nomenclature the surface layer is on the left and the deeper bulk layers are on the right [15, 16, 17,]; an alternative, reversed nomenclature has also been used by some of us previously ([18]). Several experimental and theoretical studies have found evidence that, depending on surface preparation, temperature, and oxygen pressure, other terminations may arise including substantial reconstruction where atoms of lower lying bulk layers move to the surface [4, 5, 9, 11, 12, 15, 17, 19, 20, 21, 22, 23]. One particular scenario is the vanadyl terminated V_2O_3(0001) surface, which comprises the ideal half metal layer termination V'OV, but with additional oxygen atoms (denoted O_t) atop each vanadium of the topmost layer to form a vanadyl (V=O) group [17]. This surface termination will be denoted O_tV'OV in the following text. The three intrinsic bulk terminations together with the vanadyl termination are sketched schematically in Fig. 1a. It is generally believed that the method of preparation of our epitaxial films, by evaporation of V in a partial pressure of oxygen gas, leads to a vanadyl terminated half-metal surface species. The most direct experimental evidence for this belief has come from vibrational spectroscopic studies [4, 13].

Until recently, the only information as to the V_2O_3(0001) surface termination has been based on scanning tunnelling microscopy (STM) images with atomic-scale resolution, and on theoretical total-energy calculations [15, 16, 17, 20]. Theoretical studies favour the vanadyl-covered half-metal termination model, and the STM images are believed to be consistent with this structure. The first experimental quantitative structure determination of this surface was our application of the PhD technique to this system

[18]; the results provided strong support for a half-metal termination model, with the large surface relaxations predicted by theory, but failed to resolve the question of whether or not this metal layer is terminated by the atop O_t atoms expected for a vanadyl species. Subsequently, a quantitative low-current LEED analysis has provided direct structural support for the vanadyl termination model [24], while near-edge X-ray absorption spectroscopy has also been reported to support this model [25].

Two independent investigations of the interaction of the surface of epitaxial films of V_2O_3(0001) with molecular water have been published [26, 27], and both conclude that on the as-prepared surface only molecular adsorption occurs, with no dissociation. By contrast, if the as-prepared surface is exposed to electron bombardment [26], a treatment believed to desorb vanadyl O atoms [4], or if a V-rich surface is prepared by V deposition [27], then water reacts with the surface to form surface hydroxyl species. So far the only investigation of the interaction of atomic hydrogen with a V_2O_3(0001) thin film is a thermal desorption study, in which atomic deuterium was introduced to the surface through the Pd(111) substrate crystal [28]; these experiments included measurements on films up to 5 ML thick, and showed that molecular water could be desorbed on heating, clearly implying that surface hydroxyl species were formed.

Here we present the results of a quantitative experimental investigation of the location of the O atom of hydroxyl species formed on the surface of epitaxial V_2O_3(0001) films using the technique of scanned-energy mode photoelectron diffraction (PhD), applied to the chemically-shifted component of the O 1s emission associated with surface OH species. Photoelectron diffraction exploits the coherent interference between the directly-emitted component of a photoelectron wavefield emitted from a core level of an atom and the components of the same wavefield elastically scattered by the surrounding atoms. This interference provides information on the relative position of the emitter and scatterer atoms.

In addition to the quantitative structural information, our investigation leads to several important qualitative results. Firstly, our PhD data show that the OH surface geometry is

the same for two different adsorbate preparation methods, namely reacting the surface with molecular water or with atomic hydrogen. Secondly, we find evidence for photon-assisted OH formation, due to water dissociation at the interface between the as-prepared V_2O_3(0001) film surface and a multilayer film of molecular water at low temperature (~100 K). Thirdly, we find no evidence for significant OH occupation at surface sites believed to be occupied by vanadyl O (O_t) atoms on the as-prepared surface. Finally, we report results of *ab initio* DFT cluster calculations that show that the adsorption energies of hydrogen atoms at vanadyl and at three-fold coordinated surface oxygen sites are almost identical, a result that supports aspects of the present experimental findings.

2. Experimental details and surface characterisation

The experiments were conducted in an ultra-high vacuum surface science end-station equipped with typical facilities for sample cleaning, heating and cooling. This instrument was installed on the UE56/2-PGM1 beamline of BESSY II which comprises a 56 mm period undulator followed by a plane grating monochromator [29]. Different electron emission directions can be detected by rotating the sample about its surface normal (to change the azimuthal angle) and about a vertical axis (to change the polar angle). Sample characterisation *in situ* was achieved by LEED and by soft-X-ray photoelectron spectroscopy (SXPS) using the incident synchrotron radiation. Both the wide-scan SXPS spectra for surface characterisation, and the narrow-scan O 1s spectra used in the PhD measurements, were obtained using an Omicron EA-125HR 125 mm mean radius hemispherical electrostatic analyser, equipped with seven-channeltron parallel detection, which was mounted at a fixed angle of 60° to the incident X-radiation in the same horizontal plane as that of the polarisation vector of the radiation.

The V_2O_3 (0001) films were grown on a Pd(111) substrate using methods initially characterised by the group of Netzer and coworkers [6, 7, 9] and also described by us in an earlier publication [18]. Briefly, following cleaning by cycles of 1 keV Ar^+ ion bombardment and annealing to produce clean (1x1) ordered Pd(111) surface (characterised by SXPS and LEED), the oxide films were grown from a vanadium rod

evaporator in an oxygen partial pressure of $2x10^{-7}$ mbar at a substrate temperature of ~300°C. Cooling in stages to ~150°C with the oxygen partial pressure retained, followed by heating for 1-2 minutes to ~400°C in UHV, improved the surface ordering and led to stoichiometric and well ordered V_2O_3(0001) films (with a typical thickness of 30-50 Å) as judged by SXPS and LEED.

A number of different methods were explored to produce a usable coverage of OH species on this surface. Initially, exposures to molecular water were conducted with the sample at room temperature. This approach was applied both to the as-prepared film surfaces, and to these same surfaces after exposure to electron irradiation. This treatment is believed to cause reduction of the surface vanadyl species [4], producing a bare half-metal-terminated surface, and has been reported to be necessary to achieve water dissociation at the surface [26]. Initially this electron irradiation was conducted with the electron gun in the LEED optics at an electron energy of 320 eV and a dose of ~200 μC mm^{-2} over a selected (physically scanned) area of the surface, but subsequently a biased hot filament close to the front of the sample delivered a dose about 100 times larger at an energy of 500eV, more akin to the conditions found previously to lead to sufficient surface reduction for water dissociation [26]. This electron irradiation did lead to small changes in the V 2p photoemission spectra that have been attributed to removal of the vanadyl (V=O) component, but also showed the appearance of a shoulder on the oxide O 1s photoemission peak at a chemical shift ~1.3 eV. The size of this shoulder varied significantly in different preparations; that shown in Fig. 2 after this surface treatment is particularly pronounced. Both of these spectral changes as a result of electron irradiation have been reported previously [4]. Neither the as-prepared nor the reduced surface showed significant evidence of surface OH formation as a result of the exposure to water vapour at room temperature under these conditions. However, we note that the main spectral signature of surface OH is a shoulder on the oxide O 1s photoemission peak at essentially the same chemical shift as that found after electron irradiation. Moreover, PhD spectra recorded from this O 1s component showed modulations closely similar to those obtained by successful OH dosing experiments. Therefore, we believe that our electron irradiation commonly led to some surface OH formation from dissociation of molecular

hydrogen in the residual chamber pressure even at UHV conditions. Further evidence for this conclusion was the appearance of a peak in the valence region photoemission spectrum at a binding energy of ~11 eV, also characteristic of OH.

By contrast to these unsuccessful room temperature water exposure experiments, experiments conducted by first adsorbing a multilayer of molecular water onto the surface at low temperature, and subsequently warming to remove most of the water, did lead to a significant coverage of OH species. For this experiment the water exposure was achieved using a pin-hole doser positioned ~ 1 cm in front of the sample held at a temperature of ~100 K. An exposure time of 5 min was used with a chamber pressure of $2x10^{-6}$ mbar; the pressure at the sample was undoubtedly greater than this. Fig. 2 shows representative SXPS spectra in the energy range of the O 1s photoemission peak from the V_2O_3(0001) surface under these different treatments. The spectra were recorded at a polar emission angle of 60º to enhance the surface specificity of the O 1s emission. Notice that after heating the surface, covered with a multilayer film of molecular water, to ~175 K, the resulting spectrum shows three components; the highest kinetic energy component is that from the oxide film, the next component (chemical shift -1.3 eV) is assigned to OH and the lowest kinetic energy component (chemical shift -3.0 eV) corresponds to a remaining nominal-monolayer coverage of molecular water with a chemical shift significantly less that that of the multilayer. By contrast to this result, if only one monolayer of molecular water was adsorbed onto a reduced surface at ~100 K, and then subsequently heated, no surface OH signal was obtained. The implication of these results is that significant OH is obtained on the surface by water dissociation only at the interface with a multilayer. This may occur because the residence time of H_2O on the surface is too short for effective reaction at the temperature at which the dissociation is activated. At the oxide/multilayer interface, however, the molecules are trapped and could have sufficient residence time to complete the reaction.

Also shown in Fig. 2 is the spectrum obtained after the as-prepared surface was exposed to atomic hydrogen, achieved by placing a hot filament some 5 cm from the sample and introducing H_2 gas to a pressure of $5x10^{-5}$ mbar for 2-4 min. Note that in this procedure

both sample and filament were at ground potential, so the sample was not exposed to energetic electron bombardment, as used for the surface reduction. A check on this procedure, with the filament on but no H_2 gas, failed to produce any evidence of surface OH species. This atomic H dosing treatment not only led to the shoulder on the O 1s emission seen in Fig, 2, but also to the appearance of the 11 eV binding energy state in the valence photoemission spectrum, consistent with OH formation. The total OH coverage achieved in this way was similar to, but slightly larger than, that following heating of the molecular multilayer to 200 K. Based on the relative intensity of the oxidic and OH components of the O 1s emission, and reasonable estimates of the electron attenuation length in V_2O_3 [30], the OH surface coverage obtained from multilayer water exposure and atomic H exposure, was found to be ~2.5 ML and ~3.0 ML respectively. Here we use the usual definition of 1 ML as corresponding to one atom or molecule per surface unit mesh of the substrate. In this same definition the half-metal terminated surface contains 1 ML of V atoms, and thus a fully vanadyl-terminated surface contains 1 ML of O_t atoms. Hydroxylation of all of these vanadyl O_t atoms would thus lead to an OH coverage smaller, by a factor of ~2 or 3, than that observed experimentally. This conclusion proves to be important in the light of the PhD structural results reported later in this paper.

One further significant finding in our exploration of the appropriate conditions for achieving surface OH species at the V_2O_3(0001) surface was clear evidence of photon-assisted water dissociation at the interface of the oxide and a multilayer water film. This effect occurred even on an as-prepared (unreduced) surface, and indeed, following this discovery, much of the PhD data from water-induced OH-covered surfaces was obtained from surfaces prepared in this way. Fig. 3 shows O 1s SXP spectra illustrating this effect clearly. The lower spectrum was recorded from a surface, first subjected to a multilayer water deposition at ~100 K, and then heated to ~200 K (similar to that shown in Fig. 2), this process having been monitored by photoemission. The upper spectrum was recorded immediately after the lower spectrum, but following a vertical displacement of the sample by 1.5 mm relative to the incident photon beam. Clearly there is OH on the surface where the multilayer was exposed to the synchrotron radiation beam, but not at a

different position on the surface that was exposed to the radiation only after the multilayer had been desorbed. Evidently photon-assisted OH formation occurred at the oxide/multilayer interface.

3. Data reduction and computational details

3.1 Photoelectron diffraction

PhD structural studies require the measurement of the photoemission intensity from a core level in specific directions as a function of the photoelectron energy. Modulations in the resulting spectrum arise from the change in phase of directly emitted and scattered components of the photoelectron wavefield as the photoelectron wavelength changes, and can be interpreted in terms of the scattering path lengths and thus the local geometry. In the present case the PhD modulation spectra were obtained by recording a sequence of photoelectron energy distribution curves (EDCs) around the O 1s at 4 eV steps in photon energy, in the photoelectron kinetic energy range of approximately 70-320 eV, for each of a number of different emission directions in the polar emission angle range from 0° (normal emission) to 60° in the two principle azimuthal planes, $[2\bar{1}\bar{1}0]$ and $[10\bar{1}0]$ (see Fig. 1b). Each of these data sets was processed following our general PhD methodology (see e.g. [2, 3]) in which the individual EDCs are fitted by the sum of Gaussian peaks (corresponding to the different chemically-shifted O 1s components), associated steps and a template background extracted from the high kinetic energy tails of the individual EDCs.

The intensities of the O 1s component peaks extracted in this way were then plotted as a function of kinetic energy, $I(E)$. The shape of $I(E)$ contains not only the PhD modulations, but longer period variations due to the transmission functions of the monochromator and the analyser, as well as the variation in the atomic photoionisation cross-section. These effects are approximated by fitting a spline, $I_0(E)$, through $I(E)$. The PhD modulation function, $\chi(E)$, is then given by

$$\chi(E) = \frac{I(E) - I_0(E)}{I_0(E)} \ .$$

These PhD modulation spectra form the basis of the structure determination and are compared with the results of multiple scattering simulations for trial model structures, the structures being modified until good agreement is achieved. These calculations were performed with computer codes by Fritzsche [31, 32, 33] that are based on the expansion of the final state wave-function into a sum over all scattering pathways which the electron can take from the emitter atom to the detector outside the sample. Key features are the treatment of double and higher order scattering events by means of the Reduced Angular Momentum Expansion (RAME) and inclusion (analytically) of the effects due to finite energy resolution and angular acceptance of the electron energy analyser. Anisotropic vibrations of the emitter atom and isotropic vibrations of the scattering atoms are also taken into account. The quality of agreement between the theoretical and experimental modulation amplitudes is quantified by the use of an objective reliability factor (*R*-factor) [2, 3] defined such that a value of 0 corresponds to perfect agreement and a value of 1 to uncorrelated data.

3.2 DFT cluster calculations

In our theoretical studies we consider hydrogen adsorption at the vanadyl terminated, V_2O_3(0001) surface (denoted $O_tV'OV$), where local substrate sections are simulated by finite clusters cut out from the surface region, including relaxation of the topmost surface layers [15]. Previous studies on size convergence have shown [22] that clusters as large as $V_{11}O_{34}$ sketched in Fig. 4a are already appropriate to describe electronic properties of the extended surface. Hydrogen is assumed to stabilize near two different surface oxygen sites, the terminal vanadyl site O_t and the three-fold coordinated oxygen site O_1, see Fig. 4a. Thus, we have based our simulations of hydrogen adsorption on these two model clusters $V_{11}O_{34}H$ shown in Fig. 4b, c.

The electronic structure of the surface clusters was evaluated by *ab initio* density functional theory (DFT) methods (program code StoBe [34]) using generalized gradient corrected functionals according to Perdew, Burke, and Ernzerhof (RPBE) [35, 36] to approximate electron exchange and correlation. The Kohn-Sham orbitals are represented

by linear combinations of atomic orbitals (LCAO's) using extended basis sets of contracted Gaussians from atom optimisations [37, 38]. Hydrogen binding energies are always evaluated from total cluster energy differences where atomic hydrogen was taken as the reference of the desorbed species. Corrections for basis set superposition errors (BSSE) accounting for incompleteness of the employed basis sets are likely to be small and very similar in size for the two different hydrogen adsorption sites. Therefore, they are ignored in the present calculations.

Equilibrium geometries for the two H adsorption sites were obtained within the cluster model approach by constrained optimisations, in which only the positions of the H adsorbate and of its oxygen neighbour were varied while all other atoms of the V_2O_3,(0001) surface cluster were kept fixed. Test calculations performed with different substrate interlayer spacings indicated that the H binding energy is only weakly dependent on these parameters.

4. PhD results and multiple scattering calculations

Fig. 5 shows a comparison of the experimental PhD modulations obtained from the oxide and OH components of the O 1s emission in a range of directions and for both methods of surface preparation, namely reaction at the oxide/water multilayer interface through heating of a surface to ~200 K, and atomic H reaction at room temperature. A striking feature of all of these spectra is the strong similarity of the oxide and OH PhD modulations. Indeed, bearing in mind that the modulations seen in both cases are weak, leading to significant experimental noise in the spectra, it is not clear that there are any truly significant differences between them. Comparison with similar spectra recorded from the clean as-prepared V_2O_3(0001) surface also show closely similar modulation structure. A few spectra were recorded in the same emission geometries by both preparation methods. These show some differences in the relative intensities of specific modulations, although a more significant general trend seems to be that at the higher polar emission angles, the spectra recorded from the surfaces prepared by water deposition show significantly weaker modulations than those measured from the H-dosed

surfaces, even for the oxide component. One possible reason for this is that the remaining co-adsorbed molecular water present on these surfaces comprises a disordered overlayer, and electron scattering on passage out of the surface leads to angular scrambling of the PhD modulations. Support for this view of a disordered water layer comes from the observation that PhD spectra extracted from the molecular water component of the O 1s emission show no significant modulations in any direction.

At first sight the observed strong similarity of the oxide and OH PhD spectra is very surprising. The PhD technique has been shown to have a strong sensitivity to the local structural environment of the emitter atoms, and in general we do not expect an adsorbate to adopt (almost exactly) the same local geometry as an atom in the underlying bulk. More careful consideration, however, suggests a simple qualitative interpretation. On the half-metal terminated $V_2O_3(0001)$ surface there are essentially two distinctly different possible sites for OH occupation. One is for OH to be adsorbed atop the surface V atoms of the half-metal layer (the structure shown in Fig. 4b). This could, at least in principle, arise either from H attachment to the vanadyl O atoms, O_t, see Fig. 4a, that are believed to occupy sites atop these V atoms on the as-prepared film surface, or by OH adsorption on to these V atoms if the O_t atoms have first been removed by reduction (or, indeed, if they were not present on the as-prepared film surface). The alternative possibility is that H atoms may be attached to the outermost layer under-coordinated, O_1 atoms, see Fig. 4a, each lacking one of the four V nearest neighbours that characterises their environment in the bulk solid. Evidently, these surface layer O atoms have essentially the same structural environment of neighbouring back-scatterer atoms as in the clean surface, or indeed in the underlying bulk, the only difference being associated with near-surface relaxations. Emission from these O_1 atoms may thus be expected to lead to very similar PhD modulations to those from the bulk 'oxide' O atoms.

Further qualitative and quantitative evaluation of possible OH occupation of sites atop the surface V atoms – the vanadyl sites – leads to the conclusion that such sites cannot contribute significantly to the measured OH PhD spectra. A general property of PhD is that emission along a high-symmetry near-neighbour backscattering direction typically

leads to strong modulations with a long period in photoelectron momentum (and thus energy). This appears to be particularly true for atop adsorption sites which lead to characteristic PhD spectra showing strong modulations at normal emission, the modulation amplitude falling as the polar emission angle is increased. There is no evidence for this behaviour in the spectra of Fig. 5. A quantitative test using the multiple scattering calculations confirms this conclusion, as shown in Fig. 6. Here the O 1s PhD spectra from the OH species produced by H dosing of the V_2O_3(0001) surface are compared with the results of multiple scattering simulations assuming the hydroxyl species occupy the vanadyl O sites. In this calculation the V-O bond length of the hydroxyl bonding was taken to be 1.6 Å (similar to that found theoretically for the vanadyl species and for this OH-atop configuration [17]), but calculations with values from 1.5 Å to 1.9 Å lead to similar results. The characteristic feature of all the calculations is the expected strong modulation of the normal emission spectra, and while the period of these modulations is sensitive to the bond length, the huge discrepancy with experiment is not. We should also note that far from normal emission the calculated spectra also show some sensitivity to different subsurface relaxations, but these have essentially no effect on the near-normal emission spectra. The overall *R*-factor for the full set of spectra shown in Fig. 6 is 0.93, almost exactly the value to be expected when there is zero correlation between theory and experiment.

A more promising structural model is the one based on hydroxylation of the surface layer O_1 atoms, as shown schematically in Fig. 4c. This model provides a qualitative rationale for the similarity of the oxide and OH PhD spectra. Of course, the results of these calculations can be expected to show some sensitivity to the outermost interlayer spacings near the surface. On the clean surface both theoretical studies [15] and our earlier PhD investigation [18] show clear evidence of a large (~30% or more) relaxation of the outermost vanadium-oxygen interlayer spacing (V'_1-O_1 – see Fig. 1c) relative to an ideal bulk-terminated structure. Theoretical studies indicate that the relaxation is partially reduced by the presence of vanadyl oxygen [15], and hydroxylation could lead to additional changes in these effects. We therefore exploited the automated parameter search algorithm of our multiple-scattering fitting code to determine the best-fit values,

starting from different structures. In particular, our investigation of the clean surface [18] led to two different structural models, one including the vanadyl O_t atoms, the other without. To test the idea that only the surface layer (O_1) atoms are hydroxylated we started from the set of interlayer spacings found in each of these clean surface models, although the vanadyl O atoms were omitted from the vanadyl-termination model. Optimisation of the agreement between the experimental and simulated PhD spectra from each of these starting models led to essentially identical structures, with the associated interlayer spacings being summarised in Table 1. Fig. 7 shows a comparison of the experimental and calculated PhD spectra for this structure. The overall *R*-factor value of 0.51 reflects the very significantly better agreement than that seen in Fig. 6, but nevertheless shows that this level of agreement is only modest.

Tests were also conducted on a model based on hydroxylation of both the outermost O_1 layer atoms and the vanadyl O_t atoms. The preceding discussion and the results of Fig. 6 show clearly that OH *only* in the O_1 sites is not consistent with the PhD spectra, but one might ask is some fractional occupation of this site is possible. The alternative, maximally hydroxylated, model considered corresponds to a total coverage of 4 ML of OH species, 1 ML of hydroxylated O_t atoms, and 3 ML of hydroxylated O_1 atoms. While this total coverage is somewhat larger than that observed in the experiment, the model should provide an accurate representation of the PhD spectra to be expected when 25% of the OH species occupy the vanadyl sites O_t. In this case the starting structure was the best-fit vanadyl-terminated clean surface structure of our earlier study. Somewhat strikingly, optimisation of this structure to achieve the best fit to the experimental data led to almost no improvement in the *R*-factor, the best-fit value being 0.65. This value is significantly larger than the best-fit structure with only O_1 atoms hydroxylated, and indeed the resulting simulated curves retain the strong modulations at normal emission that are characteristic of the O_t site emitters but not of the experimental data (see Fig. 7). We conclude, therefore, that any occupation of the vanadyl O sites, O_t, by OH species must be significantly less than 25%.

While these conclusions appear clear, we should comment on the high value of our

lowest *R*-factor. In typical adsorbate structure determinations involving high-symmetry adsorption sites on metal surfaces, we find best-fit *R*-factor values as low as 0.20 or even less, but for adsorbate emitter atoms in low-symmetry or multiple sites the values are usually much higher, due, in large part, to the weak modulations that make weaknesses of both experiment and theory more significant. Nevertheless, a typical criterion for an acceptable structural solution is a *R*-factor of no more than about 0.40. The value here is significantly larger (0.51), but we may also note that for our PhD study of the clean surface structure [18] our lowest overall *R*-factor was only slightly better at 0.46, and this value was derived from a set of both O 1s and V 2p PhD spectra, with one of the V 2p individual spectra yielding an *R*-factor of 0.20. The value we report here for the (OH) O 1s spectra alone is therefore better than could be achieved for the clean surface. Why are the values for both systems so poor? For the clean surface, of course, one has indistinguishable emitters in many layers with slight variations in structure due to different near-surface relaxations. For the OH emitters, however, at least when only the O_1 atoms are hydroxylated, these should all be in identical sites on a well-ordered surface. One possible problem may relate to the quality of the initial V_2O_3(0001) film surface. A sharp LEED pattern indicates good long-range order, but LEED provides information selectively on those regions of the surface that do have good long-range order. Significant areas lacking this order would have little effect on the LEED pattern, but they would contribute to the PhD signal, potentially leading to a weakening of the modulations and thus increased noise, reflected in higher minimum *R*-factors.

5. Results from DFT cluster calculations

Figs. 4b and 4c illustrate the calculated equilibrium positions of hydrogen stabilised near the terminal vanadyl site O_t, and the three-fold coordinated oxygen site O_1, respectively. Table 2 lists the values of all important geometric, electronic, and energetic parameters for these $V_{11}O_{34}$(H) clusters describing hydrogen adsorption at the V_2O_3(0001) surface.

The theoretical results clearly show that for both sites, O_t and O_1, hydrogen adsorption leads to strong chemisorptive binding, the surface OH species being formed with its

molecular axis tilted with respect to the surface normal. The calculated O-H bond lengths of about 1 Å are quite similar to typical values for OH^- radicals, a result that is consistent with the negative charges of the OH subunits obtained for the model clusters, $Q(HO_t)$ = -0.03 e and $Q(HO_1)$ = -0.21 e (e denoting the elementary charge, equal to the negative of the charge on an electron) from Mulliken analyses [39]. In addition, the V-O bond lengths at the oxygen adsorption sites, $d(O_{t,\,1}\text{-}V_1')$ in Table 2, are found to increase as a result of hydrogen adsorption. This can be explained by V-O bond weakening due to O-H bond formation at the corresponding oxygen site; this bond weakening is confirmed by the calculated Mayer bond orders, $B_M(O(n)\text{-}V_a)$, [40, 41] also listed in Table 2.

The calculated adsorption energies of hydrogen at the two oxygen sites are quite large, 3.64 eV for O_t and 3.60 eV for O_1, where atomic hydrogen is used as the reference (using molecular hydrogen ½ H_2 as the reference yields values 1.53 eV and 1.49 eV, respectively). This suggests quite strong and closely similar adsorbate binding for both sites. Formally, the calculated relative energies are inconsistent with the conclusions of the experimental PhD analysis which shows a clear preference for H adsorption at O_1 sites in the presence of O_t sites. However, taking into account the present finite cluster approximation, as well as entropic effects at finite temperatures, the calculated difference of 0.04 eV between the two adsorption energies is too small to provide a firm conclusion as to which site is energetically favourable.

6. General Discussion and Conclusions

The key result of the experiments, that is evident from even qualitative inspection of the PhD data (Fig. 5), but is fully supported by the quantitative analysis, is that hydroxylation of the $V_2O_3(0001)$ surface, whether achieved through reaction with water or with atomic H, leads almost exclusively to OH species in which the O atoms have a local backscattering geometry similar to that of atoms in the bulk oxide. Thus, few if any of the OH species occupy the sites atop surface V atoms (V'_1) that would be associated with

hydroxylation of vanadyl O_t atoms. The quantitative analysis shows that the best-fit structure corresponds to hydroxylation of the outermost (O_1) layer of (three-fold coordinated) O atoms, while Table 1 shows that most of the interlayer spacings are quite similar to those of an unrelaxed bulk termination. The notable exception is the layer spacing between the outermost V atoms (V'_1) and these hydroxylated O_1 atoms. This interlayer spacing value of 0.76 Å, with an estimated error of ±0.10 Å, is significantly less than the bulk-termination value of 0.98 Å. However, it is larger than in the clean surface for which we found, by a similar PhD data analysis, a strongly relaxed layer spacing value of 0.68 Å. An increase in the bondlength between the O_1 and both the V'_1 and V_1 atoms on hydroxylation might reasonably be expected, but the experimental result shows no significant change in $z(O_1\text{-}V_1)$. By contrast, inspection of the O_1 bondlengths in the results of the cluster calculations (Table 2) shows the main effect of hydroxylation of the O_1 atoms to be a lengthening of the $O_1\text{-}V_1$ bond. We should stress, however, that the experimental precision in determining the interlayer spacings is marginally adequate to draw any conclusions regarding changes due to hydroxylation. For completeness, Table 2 also shows the changes in the interlayer spacings obtained after hydroxylation in the cluster calculations, but we stress that these values are not comparable with the experimental values in Table 1. In particular, Table 2 shows changes in the *local* layer spacings around the single hydroxylated O atom within a cluster in which all V atoms and un-hydroxylated O atoms are fixed, whereas Table 1 corresponds to an extended surface in which the majority of the O_1 atoms are hydroxylated and there are no constraints on the resulting relaxation of any of the surface atoms.

This structural result regarding the preferred hydroxylation site may also give some insight into the reactivity of the surface. The situation is perhaps simplest for the case of reaction with atomic H. In this case it is easy to see how hydroxylation of the O_1 atoms can occur, leading to the structure shown schematically in Fig. 4c. However, the initial film surface prior to exposure to atomic H is believed to have vanadyl O_t atoms atop all the surface V'_1 atoms. Our results show clearly that few (much less than 25%), if any, OH species are formed at these sites. This seems to indicate rather clearly that the O_t atoms are not hydroxylated, assuming, of course, that they are present on the clean

surface as appears to have been established. There are, however, two other possibilities: hydroxylated vanadyl O_t atoms may react further with atomic H to produce water that is desorbed, or when the O_t is hydroxylated it no longer occupies an atop site but is displaced to a V-O bond angle relative to the surface that is essentially the same as in the bulk. In the latter case, of course, its PhD spectrum would be closely similar to that of the O_1 atoms. This second suggestion, however, is not compatible with results of the present cluster calculations which show clearly that hydroxylation of O_t does not move the oxygen atoms off their original atop position, relative to the V'_1 atom to which they are bound. This is substantiated by test calculations which confirm a local minimum for the atop site of hydroxylated O_t with barriers suggesting that O_tH diffusion is rather unlikely at moderate temperatures.

The situation for water reaction is less clear. We would expect water dissociation to lead to equal numbers of OH and H species. The H atoms can hydroxylate the O_1 atoms, but what happens to the OH? The simplest view is that these bind to V'_1 atoms, and this picture is consistent with the view already expressed in the literature that water dissociation only occurs on a surface that is V-rich, either by adding V atoms or by removing vanadyl O atoms. These V atoms are not only needed to achieve the reactivity, but also to make sites available for adsorption of the products. If the reaction starts at a fully reduced surface (all vanadyl O_t atoms removed), this description suggests that the resulting hydroxylated surface would contain equal numbers of OH species atop the V'_1 atoms (the same sites as hydroxylated vanadyl O_t atoms) and of hydroxylated O_1 atoms. Our PhD results clearly show that this is not the case; OH species atop the V'_1 atoms, if present at all, must account for significantly less than 25% of the total hydroxyl coverage. Notice that while our estimated coverage in the experiments of 2-3 ML of OH (with a precision of around 10-20%) is incompatible with occupation of only sites atop the 1 ML of V'_1 atoms, it could be compatible with 1 ML of such sites coadsorbed with 1 ML of H bonded to O_1 surface-layer oxygen atoms, corresponding to full reaction of H_2O with the bare V'_1 atoms of the fully-reduced surface. However, this model is not consistent with the PhD results. Of course, our own experiments also provide clear evidence for photon-assisted water dissociation at the oxide/ice interface, opening up the possibility of more

complex interfacial chemistry in the preparation of the hydroxylated surface from reaction with water. We should stress, though, that while we have clear evidence that photon-assisted dissociation does occur (even on the as-prepared surface), we do not have conclusive evidence that dissociation does not occur without photon assistance. In this respect our results add to, but do not conflict with, earlier reports of the reactivity of this surface to molecular water.

Our conclusion that hydrogen adsorption occurs preferentially at the 3-fold bridging O_1, rather than the terminal O_t site, at the $V_2O_3(0001)$ surface may suggest that the O_1 site is in general more reactive than O_t. This would be analogous to earlier findings for V_2O_5 surfaces for which it was argued, both on experimental [42] and theoretical [43] grounds, that bridging oxygen sites exhibit higher reactivity that terminal ones.

Acknowledgements

The authors acknowledge the financial support of the Deutsche Forschungsgemeinschaft through the Sonderforschungsbereich 546, and of the Physical Sciences and Engineering Research Council (UK), together with the award of beamtime by the BESSY synchrotron radiation facility. One of the authors (M.C.) thanks the Alexander von Humboldt Foundation for financial support.

Table 1 Summary of the outermost interlayer spacings, z, obtained from optimisation of the three initial test structures as described in the text. For comparison, the interlayer spacings for an unrelaxed bulk-terminated structure are also shown. Figures in parentheses are the values found for the two alternative best-fit structures (with and without vanadyl O atoms) found in the PhD analysis of the clean $V_2O_3(0001)$ surface [19].

model	bulk termination	hydroxylated O_1 only		hydroxylated O_1 and O_t
starting model		clean surface (non-vanadyl)	clean surface (vanadyl minus O_t atom)	clean surface (vanadyl)
R value before optimisation		0.54	0.60	0.66
R value after optimisation		0.52	0.51	0.65
$z(O_t\text{-}V'_1)$ [Å]	-	-	-	1.55
$z(V'_1\text{-}O_1)$ [Å]	0.98	0.77	0.76 (0.68)	0.68 (0.69)
$z(O_1\text{-}V_1)$ [Å]	0.98	0.94	0.97 (0.93)	0.99 (1.03)
$z(V_1\text{-}V'_2)$ [Å]	0.36	0.31	0.30 (0.35)	0.32 (0.32)
$z(V'_2\text{-}O_2)$ [Å]	0.98	1.06	1.05 (1.02)	1.07 (1.07)
$z(O_2\text{-}V_2)$ [Å]	0.98	0.98	0.98 (0.98)	0.98 (0.98)

Table 2

Calculated geometric, electronic, and energetic parameters for hydrogen adsorption at the $V_2O_3(0001)$ surface. The values refer to model clusters $V_{11}O_{34}H$ representing the oxygen sites O_t and O_1 and are compared, if needed, with results (in parentheses) for the clean surface cluster $V_{11}O_{34}$ (representing the relaxed $O_tV'OV$ surface [17]). Interatomic distances are denoted d , interlayer spacings z , atom charges, Q (from Mulliken analyses, expressed in units of the elementary charge, e), Mayer bond orders (see text) B_M. The H binding energy $E_B(H)$ at the O site is taken relative to free atomic H. Distance values d correspond to those of the relevant oxygen centre (O_t, O_1) to the nearest-neighbours V'_1, V_1 and V'_2 in the outermost layers as identified in Figs. 1 and 4.

	H at O_t	H at O_1
$d(H\text{-}O_{t,1})$ [Å]	0.980	0.983
$d(O_t\text{-}V'_1)$ [Å]	1.750 (1.586)	1.586
$d(O_1\text{-}V'_1)$ [Å]	1.880	1.870 (1.880)
$d(O_1\text{-}V_1)$ [Å]	1.934	2.078 (1.934)
$d(O_1\text{-}V'_2)$ [Å]	2.011	2.212 (2.011)
$z(O_t\text{-}V'_1)$ [Å]	1.750 (1.586)	1.586
$z(V'_1\text{-}O_1)$ [Å]	0.816	0.469 (0.816)
$z(O_1\text{-}V_1)$ [Å]	0.932	1.279 (0.932)
$z(V_1\text{-}V'_2)$ [Å]	0.341	0.341
$z(V'_2\text{-}O)$ [Å]	0.984	0.984
$\angle(H\text{-}O_t\text{-}V'_1)$ [º]	123.2	---
$\angle(H\text{-}O_1\text{-}V'_1)$ [º]	---	118.9
$\angle(H\text{-}O_1\text{-}V_1)$ [º]	---	111.2
$\angle(H\text{-}O_1\text{-}V'_2)$ [º]	---	101.7
$Q(O_{t,1})$ [e]	-0.50 (-0.25)	-0.91 (-0.66)
Q(H) [e]	0.48	0.74
$Q(HO_{t,1})$ [e]	-0.02	-0.17
$B_M(H\text{-}O_{t,1})$	0.66	0.34
$B_M(O_{t,1}\text{-}V'_1)$	1.35 (2.16)	0.71 (0.84)
$B_M(O_1\text{-}V_1)$	---	0.31 (0.60)
$B_M(O_1\text{-}V'_2)$	---	0.26 (0.44)
$E_B(H)$ [eV]	3.64	3.60

Figure Captions

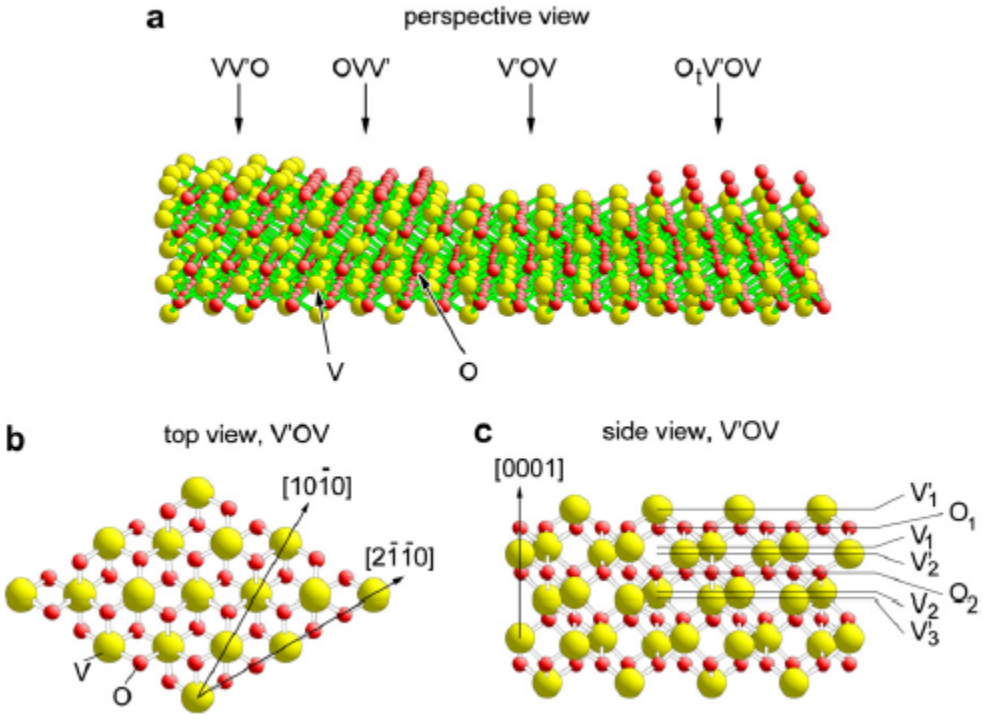

Fig. 1. Different views of the rhombohedral V_2O_3(0001) surface. The atom centres are shown by large (vanadium) and small (oxygen) balls, and are labelled accordingly. (a) Perspective view for different terminations, the full metal termination VV'O, the oxygen termination OVV', the half metal layer termination V'OV, and the vanadyl termination O_tV'OV, see text. (b) Top view of the V'OV termination showing the principal azimuthal directions used in the PhD data collection. (c) Side view of the V'OV termination. The labelling of the outermost atomic layers defines the convention used in the text and in Tables 1 and 2.

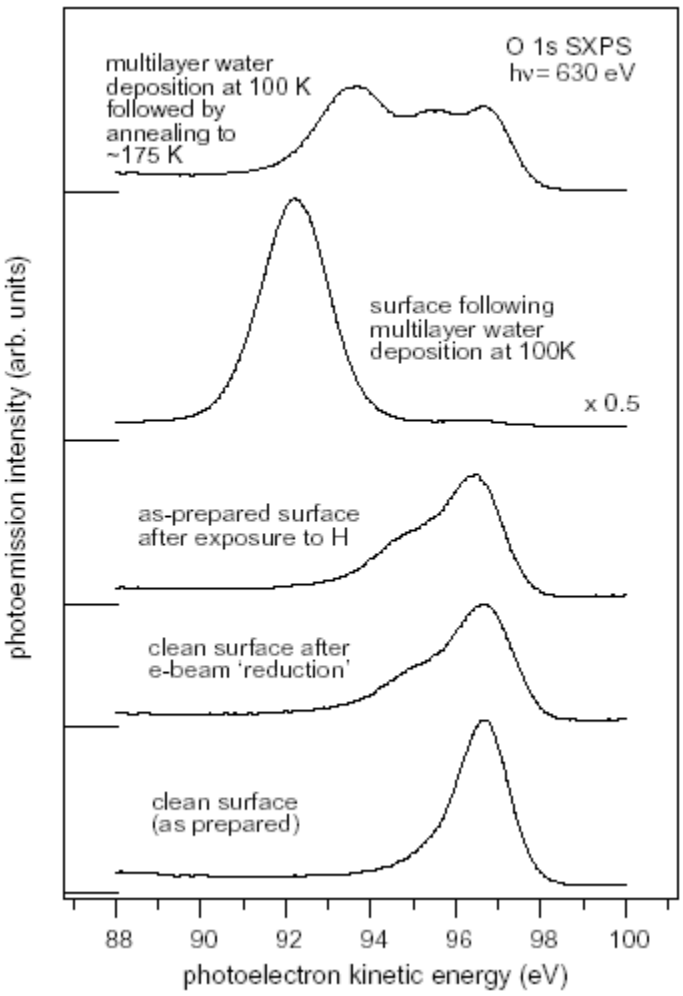

Fig. 2 Typical SXPS spectra showing the O 1s emission peak region for different surface treatments of the $V_2O_3(0001)$ film, recorded at a photon energy of 630 eV and a polar emission angle of 60º. The spectra are displaced in intensity as shown by the offset zero lines on the left.

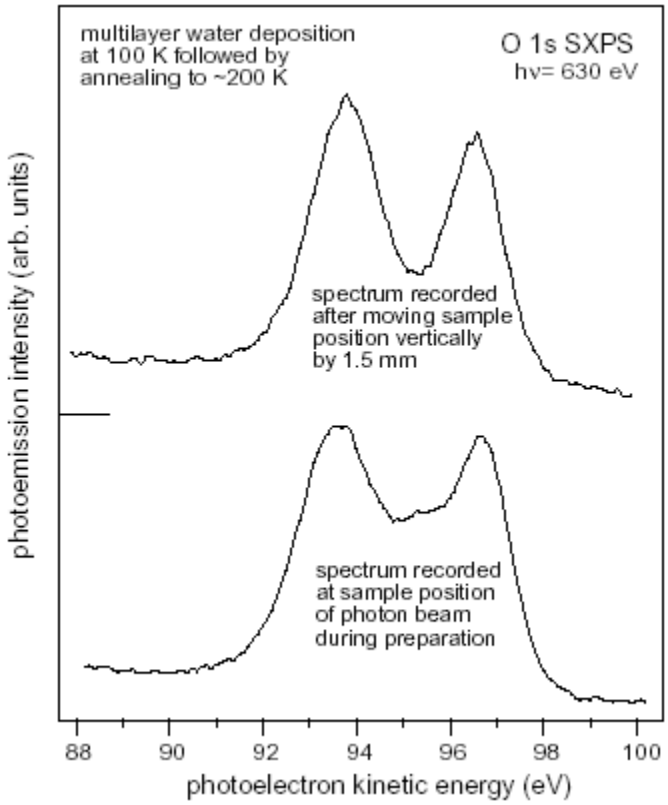

Fig. 3 SXPS spectra showing the O 1s emission peak region from a $V_2O_3(0001)$ surface covered with a water multilayer at ~100 K and then heated to ~200 K. The lower spectrum was recorded in normal emission with the sample fixed in position following monitoring of the deposition and heating sequence by photoemission. The upper spectrum was recorded after moving the sample by 1.5 mm so that the incidence flux of 630 eV photons hit a different part of the sample.

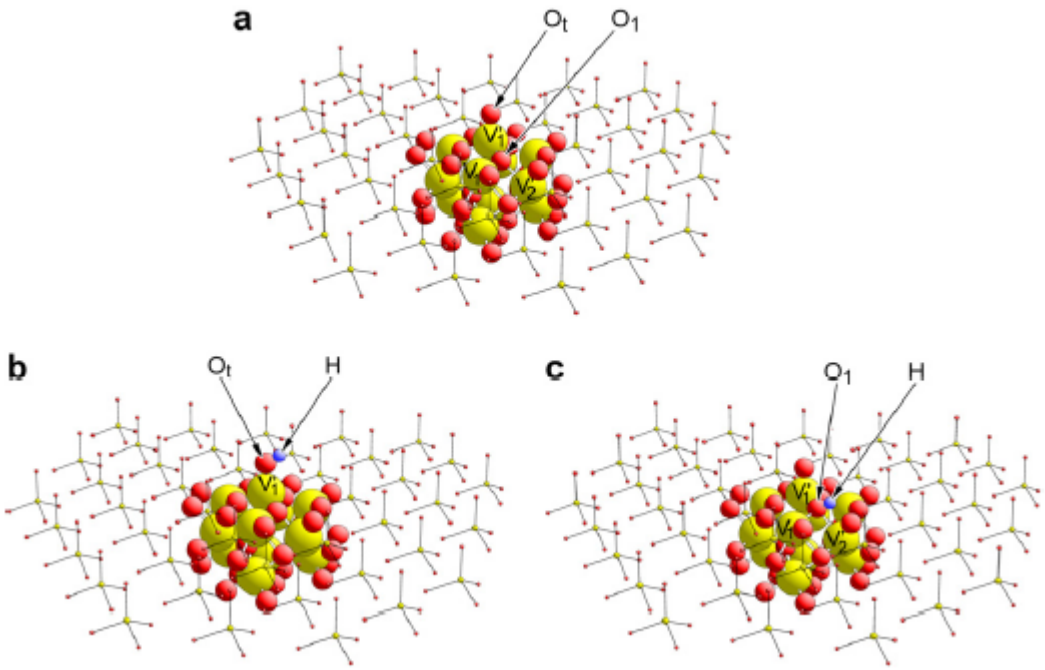

Fig. 4. Geometric structure of (a) the clean substrate cluster $V_{11}O_{34}$ representing the vanadyl terminated $V_2O_3(0001)$ surface, (b) the substrate cluster $V_{11}O_{34}H$ with hydrogen adsorbed at the vanadyl site O_t, (c) the substrate cluster $V_{11}O_{34}H$ with hydrogen adsorbed at the three-fold oxygen site O_1. The atom centres are shown by large (vanadium) and smaller (oxygen) balls and labelled accordingly, see text. To illustrate the surface environment, the clusters are shown in periodic arrangements of VO_4 units formed by the topmost vanadium centres and their four oxygen neighbours at the surface (sketched by very small balls).

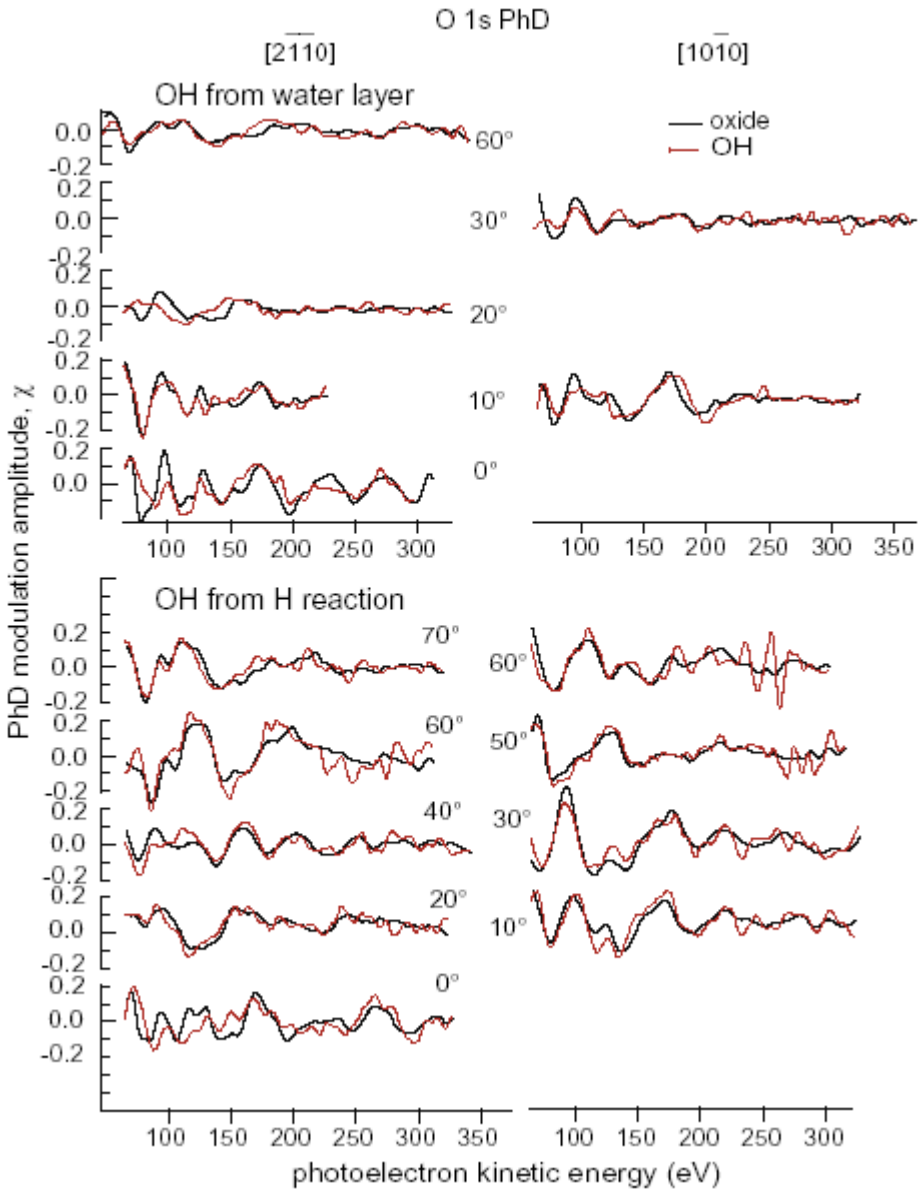

Fig. 5 Comparison of the experimental PhD spectra recorded from the OH and oxide components of the O 1s emission, from OH-covered surfaces prepared by the two alternative methods, in a range of different emission geometries as specified by the azimuth and polar angle.

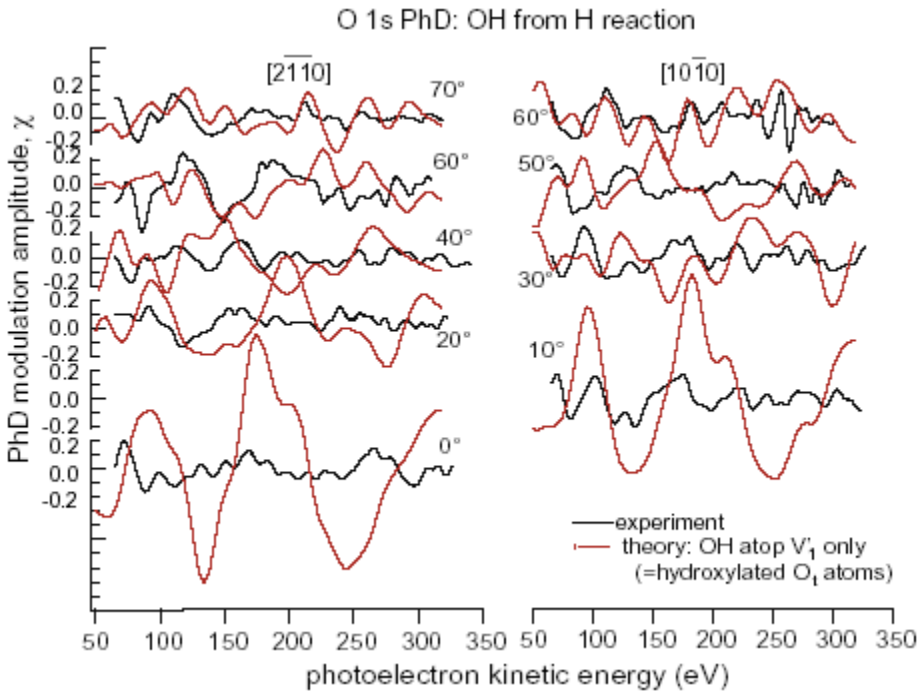

Fig. 6 Comparison of the experimental O 1s (OH) PhD spectra from the H-dosed $V_2O_3(0001)$ surface with the results of multiple scattering calculations assuming the hydroxylated emitter O atoms are atop the outermost layer V'_1 atoms (equivalent to hydroxylated vanadyl O_t atoms, see Fig 4b).

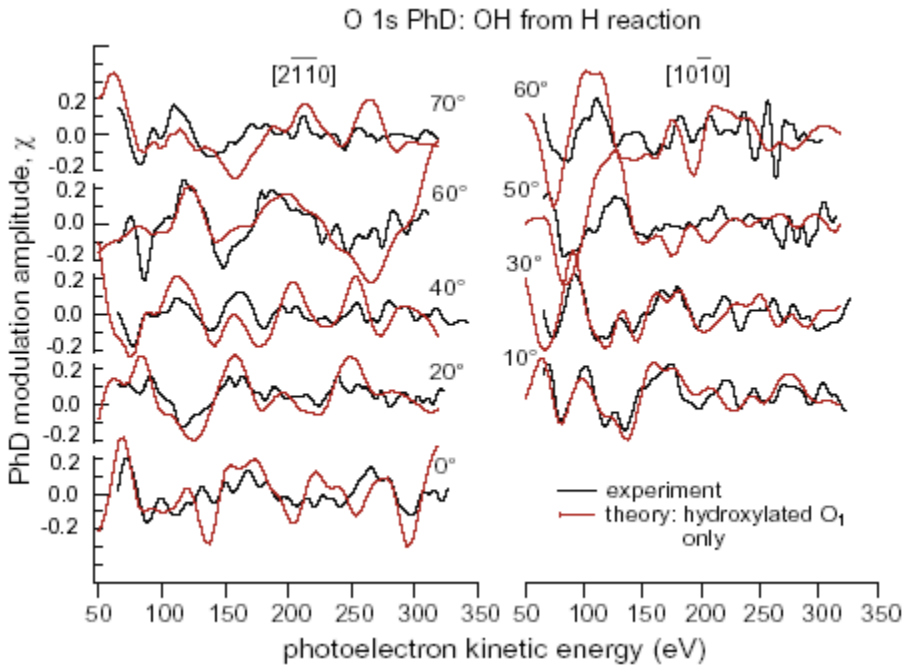

Fig. 7 Comparison of the experimental O 1s (OH) PhD spectra from the H-dosed $V_2O_3(0001)$ surface with the results of multiple scattering calculations assuming the emitter atoms are hydroxylated O_1 atoms (see Figs. 1 and 4c).

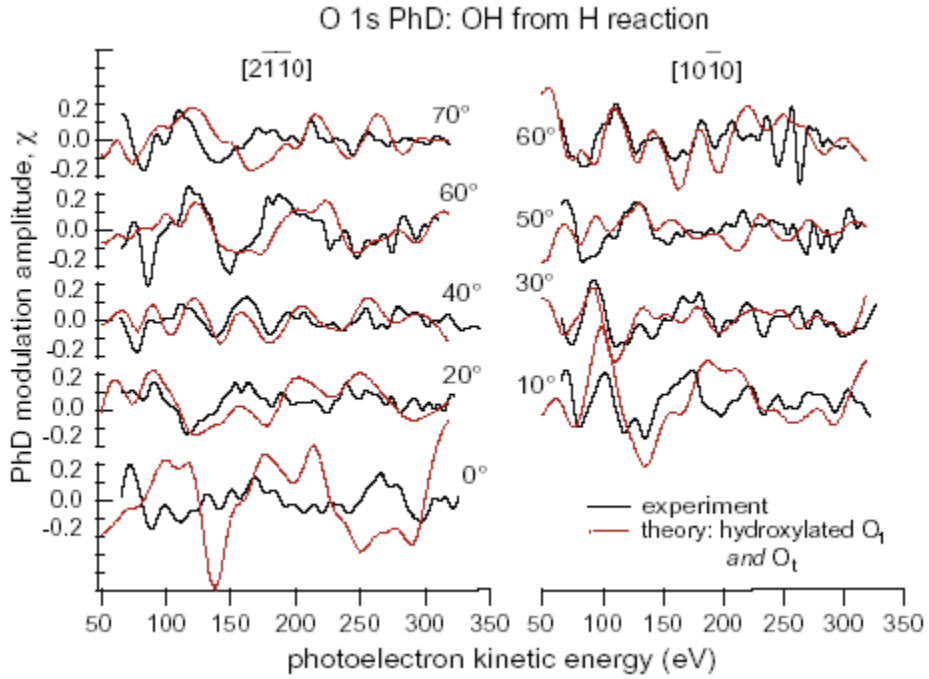

Fig. 8 Comparison of the experimental O 1s (OH) PhD spectra from the H-dosed $V_2O_3(0001)$ surface with the results of multiple scattering calculations assuming the emitter atoms are both hydroxylated O_1 atoms and OH species atop the V'_1 atoms (i.e.

equivalent to hydroxylated vanadyl O_t atoms). In this model the ratio of O_l to O_t (hydroxylated) emitter atoms is 3:1.

References

1 B. Grzybowska-Świerkosz, F. Trifirò, J. C. Vedrine (eds) *Vanadia catalysts for selective oxidation of hydrocarbons and their derivatives*, Appl. Catal. A 157 (1997) 1.

2 D. P. Woodruff, A. M. Bradshaw, Rep. Prog. Phys. 57 (1994) 1029.

3 D. P. Woodruff, Surf. Sci. Rep. 62 (2007) 1.

4 A. –C. Dupuis, M. Abu Haija, B. Richter, H. Kuhlenbeck, H. –J. Freund, Surf. Sci. 539 (2003) 99.

5 H. Niehus, R. -P. Blum, D. Ahlbehrendt,Surf. Rev. Lett., 10 (2003) 353 .

6 F. P. Leisenberger, S. Surnev, L. Vitali, M. G. Ramsey, F. P. Netzer, J. Vac. Sci. Technol. A 17 (1999) 1743.

7 S. Surnev, L. Vitali, M. G. Ramsey, F. P. Netzer, G. Kresse, J. Hafner, Phys. Rev. B 61 (2000) 13945.

8 S. Surnev, G. Kresse, M. G. Ramsey, F. P. Netzer, Phys. Rev. Lett. 87 (2001) 86102.

9 S. Surnev, G. Kresse, M. Sock, M. G. Ramsey, F. P. Netzer, Surf. Sci. 495 (2001) 91.

10 C. Klein, G. Kresse, S. Surnev, F. P. Netzer, M. Schmid, P. Varga, Phys. Rev. B 68 (2003) 235416.

11 J. Schoiswohl, M. Sock, S. Eck, S. Surnev, M. G. Ramsey, F. P. Netzer, Phys. Rev. B 69 (2004) 155403.

12 J. Schoiswohl, M. Sock, S. Surnev, M. G. Ramsey, F. P. Netzer, G. Kresse, J. N. Andersen, Surf. Sci. 555 (2004) 101.

13 F. Pfuner, J. Schoiswohl, M. Sock, S. Surnev, M. G. Ramsey, F. P. Netzer, J. Phys.: Condens. Matter 17 (2005) 4035.

14 P. D. Dernier, J. Phys. Chem. Solids 31 (1970) 2569.

15 I. Czekaj, K. Hermann, M. Witko, Surf. Sci. 525 (2003) 33.

16 I. Czekaj, M. Witko, K. Hermann, Surf. Sci. 525 (2003) 46.

17 I. Czekaj, K. Hermann, M. Witko, Surf. Sci. 545 (2003) 85.

18 E. A. Kröger, D. I. Sayago, F. Allegretti, M. J. Knight, M. Polcik, W. Unterberger, T. J. Lerotholi, K. A. Hogan, C. L. A. Lamont, D. P. Woodruff, Surf. Sci. 601 (2007) 3350.

19 G. Kresse, S. Surnev, M. G. Ramsey, F. P. Netzer, Surf. Sci. **492** (2001) 329.

20 G. Kresse, S. Surnev, J. Schoiswohl, F. P. Netzer, Surf. Sci. 555 (2004) 118.

21 H. Niehus, R. P. Blum, D. Ahlbehrendt, Physica Status Solidi **A 187** (2001) 151.

22 S. Surnev, M. G. Ramsey, F. P. Netzer, Prog. Surf. Sci. **73** (2003) 117.

23 T. K. Todorova, M. V. Ganduglia-Pirovano, J. Sauer, J. Phys. Chem. **B 109** (2005) 23523.

24 Y. Romanyshyn, H. Kuhlenbeck, H. –J. Freund, to be published.

25 C. Kolczewski, K. Hermann, S. Guimond, H. Kuhlenbeck, H. –J. Freund, Surface Sci. 601 (2007) 5394.

26 M. Abu Haila, S. Guimond, A. Uhl, H. Kuhlenbeck, H. –J. Freund, Surf. Sci. 600 (2006) 1040.

27 J. Schoiswohl, G. Tzvetkov, F. Pfuner, M. G. Ramsey, S. Surnev, F. P. Netzer, Phys. Chem. Chem Phys. 8 (2006) 1614.

28 M. Kratzer, S. Surnev, F. P. Netzer, A. Winkler, J. Chem. Phys. 125 (2006) 074703.

29 K. J. S. Sawhney, F. Senf, M. Scheer, F. Schäfers, J. Bahrdt, A. Gaupp, W. Gudat, Nucl. Instrum. Methods A 390 (1997) 395.

30 C. J. Powell, A. Jablonski, *NIST Electron Effective-Attenuation-Length Database*, NIST Standard Reference Database 82, NIST, Gathersburg, USA (2003).

31 V. Fritzsche, J. Phys.: Condens. Matter 2 (1990) 1413.

32 V. Fritzsche, Surf. Sci. 265 (1992) 187.

33 V. Fritzsche, Surf. Sci. 213 (1989) 648.

34 The program package StoBe is a modified version of the DFT-LCGTO program package deMon, originally developed by A. St.-Amant and D. Salahub (University of Montreal), with extensions by L. G. M. Pettersson and K. Hermann.

35 J.P. Perdew, K. Burke, M. Ernzerhof, Phys. Rev. Lett. 77 (1996) 3865.

36 B. Hammer, L. B. Hansen, J. K. Norskov, Phys. Rev. B 59 (1999) 7413

37 “Density Functional Methods in Chemistry”, eds. J. K. Labanowski, J. W. Anzelm, Springer -Verlag, New York 1991.

38 N. Godbout, D. R. Salahub , J. Andzelm, E. Wimmer, Can. J. Phys. 70 (1992) 560.

39 R. S. Mulliken, J. Chem. Phys. 23 (1955) 1833, 1841, 2388, 2343.

40 I. Mayer, Chem. Phys. Lett. 97 (1983) 270.

41 I. Mayer, J. Mol. Struct. (Teochem) 149 (1987) 81.

42 J. Haber, in C. Mortena, A. Zecchina, and G. Costa (eds.), "Structure and Reactivity of Surfaces", Elsevier, Amsterdam, 1989.

43 M. Witko, K. Hermann, J. Mol. Catal. 81 (1993) 279.